THE JOURNAL OF PHYSICAL CHEMISTRY B

Article

pubs.acs.org/JPCB

Quantum Yield of Charge Separation in Photosystem II: Functional Effect of Changes in the Antenna Size upon Light Acclimation

Emilie Wientjes,[||,†] Herbert van Amerongen,[‡,§] and Roberta Croce*[,†]

[†]Department of Physics and Astronomy, Faculty of Sciences, VU University Amsterdam, 1081 HV Amsterdam, The Netherlands

[‡]Laboratory of Biophysics, Wageningen University, 6703 HA Wageningen, The Netherlands

[§]MicroSpectroscopy Centre, 6703 HA Wageningen, The Netherlands

ABSTRACT: We have studied thylakoid membranes of *Arabidopsis thaliana* acclimated to different light conditions and have related protein composition to excitation energy transfer and trapping kinetics in Photosystem II (PSII). In high light: the plants have reduced amounts of the antenna complexes LHCII and CP24, the overall trapping time of PSII is only ∼180 ps, and the quantum efficiency reaches a value of 91%. In low light: LHCII is upregulated, the PSII lifetime becomes ∼310 ps, and the efficiency decreases to 84%. This difference is largely caused by slower excitation energy migration to the reaction centers in low-light plants due to the LHCII trimers that are not part of the $C_2S_2M_2$ supercomplex. This pool of "extra" LHCII normally transfers energy to both photosystems, whereas it transfers only to PSII upon far-red light treatment (state 1). It is shown that in high light the reduction of LHCII mainly concerns the LHCII-M trimers, while the pool of "extra" LHCII remains intact and state transitions continue to occur. The obtained values for the efficiency of PSII are compared with the values of F_v/F_m, a parameter that is widely used to indicate the PSII quantum efficiency, and the observed differences are discussed.

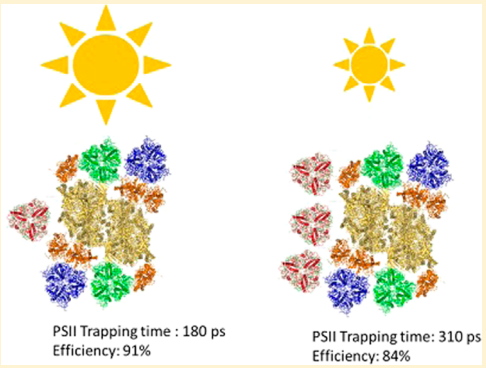

INTRODUCTION

In oxygenic photosynthesis, the thylakoid membrane-embedded supercomplexes Photosystem II (PSII), cytochrome b_6f and Photosystem I (PSI) work in series to oxidize water, reduce NAD(P)$^+$ to NAD(P)H, and generate a proton gradient over the membrane. The proton gradient drives the synthesis of ATP by the ATP synthase. NAD(P)H and ATP are used in the Calvin cycle, which ultimately leads to the synthesis of carbohydrates. The driving force for these reactions is light absorbed by the pigments of PSI and PSII; see, for example, ref 1. Both photosystems consist of a core complex and an external light-harvesting system. Photochemistry takes place in the core complex, which harbors the reaction center (RC) where charge separation occurs, the electron transport cofactors, and the internal antenna complexes CP43 and CP47, which coordinate chlorophyll *a* (Chl *a*) and *β*-carotene.[2] The core complexes are rather complicated and expensive pieces of machinery, and to supply them with enough energy in higher plants and algae, a cost-effective outer light-harvesting complex (Lhc) has appeared during evolution with an extremely high pigment to protein ratio: 15 kDa of pigment per 25 kDa of protein. This makes a monolayer of Lhc's able to absorb around 2% of the incident light. The pigments associated with Lhc's are Chl *a*, Chl *b*, and carotenoids: lutein, violaxanthin, neoxantin, and *β*-carotene.[3] Higher plant PSI coordinates four Lhc's (Lhca1-4), which are present in a one-to-one ratio with the core, independent of the grow-light intensity.[4,5] The outer antenna system of PSII is composed of 6 Lhcb's. Various combinations of Lhcb1, Lhcb2, and Lhcb3 form the major trimeric LHCII complexes, while Lhcb4 (CP29), Lhcb5 (CP26), and Lhcb6 (CP24) associate with the PSII core as monomeric complexes reviewed in ref 6. The minimal size of the PSII supercomplex is a dimer of the core (C) associated with two CP26s, two CP29s, and two strongly (S) bound LHCII trimers (C_2S_2).[7] The largest supercomplex observed in *Arabidopsis thaliana* is $C_2S_2M_2$, which in addition associates two CP24s and two moderately (M) bound LHCII trimers.[6,8] Up to two more LHCII trimers can be present per PSII RC in plants, for example,[9,10] but so far their position with respect to the PSII supercomplex is not known. Only in spinach one copy on an additional trimer (named L, loosely bound) was observed associated with the dimeric supercomplex in a specific position.[11] In the following, we call "extra" all trimers that are not S and M. We prefer to use this definition instead of dividing the trimer in L and "extra" as done in spinach[11] because in *Arabidopsis* trimer L was never observed and not all "extra" trimer can be associated with the supercomplex in the L position. A fraction of the LHCII trimers can move between PSI and PSII during state transitions,[12] and it has been shown that this fraction belongs to the "extra" LHCII pool.[13,14] The migration of LHCII from PSII to PSI has

Special Issue: Rienk van Grondelle Festschrift

Received: February 16, 2013
Revised: March 26, 2013
Published: March 27, 2013

long been considered a short-term acclimation process that occurs when PSII is overexcited with respect to PSI. However, we have recently shown that LHCII is also part of the PSI antenna system in long-term acclimated plants.[14]

The function of the outer antenna system is to capture enough light to drive photochemistry efficiently under light-limited conditions; however, the light intensity that plants experience fluctuates during seasons, days, and even minutes/seconds. When more light energy is absorbed than can be used for photosynthesis, the electron transport chain will be blocked. In the Lhc's of PSII, this leads to longer ^{1}Chl *a* excited-state lifetimes, which increase the probability of triplet state (^{3}Chl*) formation. ^{3}Chl* can react with molecular oxygen to form the highly reactive singlet oxygen ($^1O_2$), which can oxidize pigments, lipids, and proteins and lead to photoinhibition of PSII.[15] In the Lhc's, the chlorophylls are protected by nearby carotenoids, which quench ^{3}Chl* and scavenge $^1O_2$.[16−19] In the RC, however, charge recombination leads to the formation of triplets on the primary electron donor,[20] which cannot be scavenged by a nearby carotenoid, therefore leading to the enhanced formation of $^1O_2$.

In plants, several protection mechanisms have evolved. On a short time scale the plants respond by activating emergency regulatory mechanisms, which are not meant to ensure high efficiency, but mainly to avoid photodamage. These mechanisms involve reorganization of existing membrane complexes, which leads to redirection or quenching of the excess absorbed energy.[21−23] In the long term, plants respond by redesigning the photosynthetic apparatus, by changing the protein composition, for example.[24] An important long-term response is the modulation of the PSII antenna size to adjust the PSII excitation pressure.[25−27] In high light, the antenna size is decreased by reduction of the CP24, Lhcb1, and Lhcb2 levels with respect to normal light conditions (typically 100−150 μmol/m^2/s for *Arabidopsis thaliana*), while the levels of Lhcb1 and Lhcb2 are increased in low light.[5,28]

The quantum efficiency of charge separation in PSII is given by: $\Phi_{CS} = 1 - \tau_{avg}/\tau_{Chl}$, where τ_{avg} and τ_{Chl} are the average lifetime of an excited state in PSII in the presence and (hypothetical) absence of charge separation. The average PSII lifetime (τ_{avg}) can be considered as the sum of two contributions, $\tau_{avg} = \tau_{trap} + \tau_{mig}$, in which τ_{trap} represents the trapping time of an equilibrated system, which scales linearly with the number of more or less isoenergetic pigments. The migration time τ_{mig} represents the average time it takes for an excitation to reach the primary donor for the first time and represents in fact the equilibration time reviewed in ref 29. When the PSII antenna size increases in low light, the excited-state lifetime also increases. This leads to lower charge-separation efficiency, which implies that there must be a trade-off between the increased light-harvesting capacity and the light-harvesting efficiency.

In this work, we have studied light-harvesting in the thylakoid membranes of *Arabidopsis thaliana* plants grown in different light conditions. The aim is to understand the effect of changes in the antenna composition and size on the overall trapping time and efficiency of the system.

EXPERIMENTAL METHODS

Plant Material − *Arabidopsis thaliana*. (Col) WT plants were grown at an 8 h light/16 h dark regime at a light intensity of 100 μmol photons m^{-2} s^{-1}, 70% humidity, and 22 °C (Plant Climatics Percival Growth Chamber, model AR-36L, Germany). After 4 weeks, normal-light WT plants (NL) plants were grown an additional 2.5 weeks at this light intensity, while low-light (LL) and high-light (HL) plants were transferred to 20 μmol photons m^{-2} s^{-1} and 800 μmol photons m^{-2} s^{-1} (for LL and HL, growth chamber models were AR-36L and SE 1100), respectively, for an additional 4 weeks. Thylakoids were isolated from plants brought to State 1 (St1) by treatment with 50 min of 20 μmol photons m^{-2} s^{-1} 450 nm LED light + far red light (747 nm, 28 nm full width at half-maximum, 6 μmol photons m^{-2} s^{-1}) in a Fytoscope FS130 apparatus (Photon Systems Instruments, Brno, Czech Republic) or from plants treated with 6 to 7 h of daylight (further referred to as light-adapted). Thylakoid isolation was performed as in ref 8 (until the solubilization step), and all buffers were supplemented with 10 mM NaF to inhibit phosphatase activity.

Polyacrylamide Gel Electrophoresis and Western Blot Analysis. Denaturing PAGE was performed with the Tris-Tricine system[30] at a 14.5% acrylamide concentration. To estimate the level of Lhcb1,2 per CP29, we digitized the gels with a Fujifilm LAS 300 scanner after Coomassie Brilliant Blue staining, and the optical density integrated over the area of the band was quantified using the GEL-PRO Analyzer (Media Cybernetics). The number of Lhcb1,2 monomeric subunits per PSII core was quantified as in ref 31. Blue-native PAGE was performed as in ref 32, with the 25BTH20G buffer and an acrylamide/bisacrylamide ratio of 32:1 in both stacking (3.5%) and resolving (4 to 14%) gel. The final Chl concentration was 0.5 mg/mL, and the final detergent concentration was 1% α-*n*-dodecyl-D-maltoside; 8 μg of Chl was loaded per lane. Western blot analysis was performed against CP43 and CP24 with antibodies from Agrisera (Sweden) as in ref 33. The blots were digitized with a Fujifilm LAS 3000 scanner and the optical density integrated over the area of the band was quantified using a GEL-PRO analyzer (Media Sybernetics, Inc., Silver Spring, MD, USA). The NL samples are presented for four different Chl quantities to confirm that the signal is linear with the sample quantity. The ratio of the CP24/CP43 band intensities was normalized to 100% (with a standard deviation of 15%, n = 4) for NL plants and compared with the ratios obtained for the HL (55 ± 5%) and LL (112 ± 16%) plants.

PSI/PSII and Chl *a*/*b* Ratio. The PSI/PSII ratio was estimated from the carotenoid electrochromic shift.[34−36] Kinetic measurements were performed using the JTS-10 Joliot-type spectrometer on intact dark-adapted leaves[37] (BioLogic, France). A saturating flash was provided by a xenon flashlamp (3 μs full width at half-maximum), and measuring flashes were provided with a white LED source passed through an interference filter (520 and 546 nm). PSI and PSII charge-separation capacity was calculated from changes in the amplitude of the fast phase (100 μs after saturating flash) of the ECS signal at 520 nm (corrected for the small changes at 546 nm) upon excitation with a saturating flash, before (PSI+PSII signal) and after (PSI signal) infiltration of the leaves with PSII inhibitors (200 μM DCMU and 1 mM hydroxylamine). Infiltration with DCMU and hydroxylamine led to a F_v/F_m value <0.02, showing that PSII was successfully inhibited. The Chl *a*/*b* ratio of the thylakoids was evaluated by fitting the absorption spectra of the 80% acetone extracts with the spectra of the individual pigments, as previously described.[38]

State Transitions Measurement. Chlorophyll fluorescence of attached leaves was measured with the Dual PAM-100 apparatus (Walz, Germany). The plants were dark-adapted.

dx.doi.org/10.1021/jp401663w | J. Phys. Chem. B 2013, 117, 11200−11208

Table 1. Characteristics of WT Plants Acclimated to LL, NL, and HL Plants

	F_v/F_m[a]	Chl a/b[b]	PSI/PSII[c]	Lhcb1,2/PSII RC[d]	Lhcb3/PSII RC[e]	LHCII trimer/PSII RC[f]	LHCII trimer/PSII RC[g]	"extra" LHCII[h]	Chls a/PSII RC[i]
LL	0.79	2.95	0.71	8.34 (0.38)	1	3.1	3.1	1.1	127
NL	0.82	3.33	0.75	6.17 (0.47)	1	2.4	2.4	0.4	111
HL	0.80	3.67	0.65	5.96 (0.33)	0.55	2.2	1.7	0.2–0.65	96–105

[a]Standard deviation (SD) ≤ 0.02, $n \geq 4$. [b]SD ≤ 0.05, $n \geq 3$. [c]SD = 0.03, $n \geq 6$. [d]Lhcb1,2 per PSII RC determined from SDS-PAGE gel; SD is indicated between brackets, $n \geq 3$. [e]Level of Lhcb3 per PSII RC. (See the text.) [f]Number of LHCII trimers per PSII RC based on (Lhcb1,24+Lhcb35)/3. [g]LHCII trimers per PSII RC calculated based on the Chl a/b ratio, the PSI/PSII ratio, and the pigment composition of PSI and the components of PSII; see ref 31. [h]LHCII trimers outside the PSII supercomplex based on 2 LHCII trimers per PSII RC in the C2S2M2 supercomplex under NL and LL and 1.55 in C2S2M2/C2S2M1/C2S2 supercomplexes under HL, where the level of CP24 and thus trimer-M is decreased. (See the text.) [i]Number of Chls a associated with PSII (core +antenna), based on the pigment composition of the components; see ref 31.

The actinic-light illumination was provided with 635 nm LEDs, the intensity was 22 μmol photons m^{-2} s^{-1}, and the far-red intensity was 125 μmol photons m^{-2} s^{-1}. The maximum fluorescence F_m was determined using a 0.5 s saturating pulse (6000 μmol photons m^{-2} s^{-1}). In State 2 (St2), F_{m2} was measured after 15 min of illumination with actinic light, and in St1, F_{m1} was measured after 25 min of illumination with far-red light (or 10 min without actinic light). (See Figure 2.) The F_{m1} and F_{m2} values measured in the presence of actinic light were used to calculate the state transition parameter $qT = (F_{m1} - F_{m2})/F_{m1}$, which reflects changes in the PSII cross section.

Time-Correlated Single Photon Counting. Time-resolved fluorescence of thylakoids was measured by time-correlated single photon counting (TCSPC). Measurements were performed at 290 K in 10 mM Hepes pH 7.5, 5 mM $MgCl_2$, 15 mM NaCl, and 10 mM NaF with a home-built setup, as previously described.[39] Excitation was performed with a ~0.2 ps light pulse at 440 or 475 nm and a repetition rate of 3.8 MHz. Other experimental settings were as in ref 9. The steady-state fluorescence emission spectra were measured after excitation at 440 or 475 nm on a Spex Fluorolog 3.2.2 apparatus (HORIBA Jobin-Yvon, USA) and used to calibrate the decay-associated spectra (DAS).

Theory of Fluorescence Kinetics. The average PSII lifetime can be considered as the sum of τ_{trap} and τ_{mig}. τ_{trap} is the charge-separation time (τ_{CS}) divided by the probability that the excitation is located on the RC. For more or less iso-energetic pigments: $\tau_{trap} = N_{eff}*\tau_{CS}$, with $N_{eff} = N_{PSII}/N_{RC}$, where N_{PSII} and N_{RC} are the number of Chl a molecules in PSII and the RC, respectively.[40,41] Per PSII RC, there is one core complex (containing one CP43 and one CP47), one CP24 (0.55 for HL plants), one CP26, one CP29, and number (n) of LHCII trimers. For NL and LL plants, the number of Chl a molecules per RC is given by: no. Chl $a = 53 + 24n$.[42] For HL plants, this number was corrected for the lower amount of CP24 (coordinating five Chl a[43]). The PSII RC contains six Chls a.[44] If charge separation is reversible, as is the case in PSII,[42,45] then also the secondary charge separation time (τ_{RP}) and the drop in free energy (ΔG) should be taken into account. If, in addition, the excited-state decay processes in the antenna are considered, then the equation changes into: $\tau_{trap} = 1/\{(1/(N_{eff}[\tau_{RP} \exp(-\Delta G/(kT))]) + (1/\tau_{Chl})\}$, with τ_{Chl} the Chl excited state lifetime in the absence of charge separation. For further details, see ref 9.

RESULTS

Plants were acclimated for several weeks to low light (LL, 20 μmol photons m^{-2} s^{-1}), normal light (NL, 100 μmol photons m^{-2} s^{-1}), or high light (HL, 800 μmol photons m^{-2} s^{-1}). The parameter F_v/F_m is, in general, used to evaluate the PSII fitness, and it is assumed to be the quantum efficiency of PSII. This value is usually ~0.8, but when PSII is photoinhibited it can decrease below 0.4.[46,47] F_v/F_m was close to 0.8 for all of our plants (Table 1), indicating that PSII was functional.

LHCII Content per PSII RC. It is generally accepted that in response to different light intensities the PSII antenna size changes to optimize light harvesting.[25−27] To evaluate the extent of these changes, we determined the level of Lhcb1,2 per CP29 in the membranes of plant grown in different light intensities by denaturing SDS-PAGE (Figure 1A). Because CP29 and PSII RC are present in a one-to-one ratio,[7] this also provides the level of Lhcb1,2 per PSII RC. In addition to the level of LHCII, it has been reported that also the level of CP24 can be reduced in HL;[5] indeed Western blotting analysis

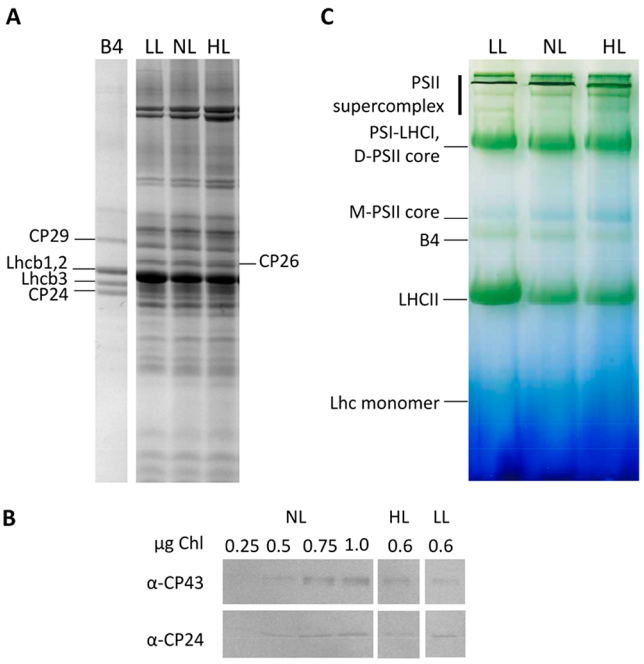

Figure 1. Protein composition of the thylakoid membranes of LL, NL, and HL plants. (A) Tris-tricine denaturing SDS-PAGE. The increase in Lhcb1 and 2 in LL is directly visible in the gel. (B) Western blot analysis of CP24 content per CP43 (and therefore per PSII core) of NL, HL, and LL thylakoids. The NL sample was loaded at four different Chls concentrations (as indicated) to confirm that the signal is linear with the concentration; 0.6 μg Chl of HL and LL samples were loaded. (C) Blue-native PAGE. The identity of the different photosynthetic supercomplexes (based on the second dimension gel, not shown) is indicated. M- and D-PSII core indicate monomer and dimer. B4 is the subcomplex composed of trimer M/CP29/CP24.

showed that in our plants the level of CP24 per PSII was 55% (the standard deviation was 5%, $n = 3$) in HL as compared with NL and LL plants (Figure 1B). In the absence of CP24, trimer-M cannot associate with the PSII supercomplex.[8,48] In agreement with this, it was found that Lhcb3, which is mostly or exclusively present in trimer M,[49,50] is reduced to a similar extent as CP24.[51] Taking into account that one trimer-M coordinates one Lhcb3,[50] it can be concluded that 0.55 Lhcb3 subunits are present per PSII RC in HL plants, while there is 1 Lhcb3 per RC in LL and NL plants, where all PSII supercomplexes are of the $C_2S_2M_2$ type.[51] These data were used to calculate the number of LHCII trimers per PSII RC (Table 1). In parallel, the number of LHCII trimers per PSII RC was assessed based on the PSI/PSII ratio, the Chl a/b ratio, and the pigment composition of the individual PSI and PSII complexes; see the Experimental Methods and ref 31. Both methods give rather similar results (Table 1). In conclusion, LHCII levels are reduced in HL plants (1.7 to 2.2 trimers per PSII RC) and increased in LL plants (3.1) as compared with NL plants (2.4). We notice that although the trend is in line with the expectation, the number of LHCII trimers in NL is lower than that in a previous report (9). We do not have a clear explanation for this. Probably in addition to light intensity other factors play a role in shaping the antenna size of PSII. However, the analysis of these effects is out of the scope of the present paper.

LHCII trimers can be divided into two pools: those associated with the PSII core, which are part of the PSII supercomplex (i.e., LHCII-S and LHCII-M), and the "extra" trimers that are not part of the supercomplex. Our data allow to discriminate between these two pools. The level of extra LHCII is the highest for LL plants, whereas lower amounts are found for NL and HL plants (Table 1). This is supported by the blue-native gel results (Figure 1C), showing a strong LHCII band for LL plants when compared with HL and NL. The amounts for NL and HL plants are similar. The native gel also shows that in HL the amount of the complex composed of CP29/CP24/LHCII trimer M (indicated as B4 in the Figure) is decreased compared with LL and NL, in agreement with a reduced amount of CP24 and Lhcb3.

State Transitions. It was recently reported that field-grown plants, with strongly reduced amounts of LHCII, still have a high capacity of performing state transitions, while the capacity was reduced in LL plants.[52] We measured the ability of our LL, NL, and HL plants to perform state transitions using the qT parameter. (See the Experimental Methods.) Figure 2 shows that the qT values are high under all growth conditions, and although the data might seem to indicate that qT becomes slightly smaller with decreasing antenna size, the values are not significantly different (student's t test, $p > 0.05$). Thus, even though the size of the LHCII pool is decreased in HL plants, the capacity to perform state transitions still exists. This nicely fits with the fact that the reduction of the PSII antenna size in HL plants as compared with NL plants is mainly coming from the decrease in the PSII supercomplex size, whereas the pool of "extra" LHCII is retained.

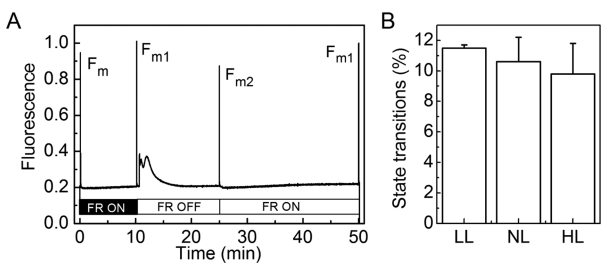

Figure 2. State transitions. (A) Example of fluorescence trace of a NL plant; the bar shows if the actinic light is off (black) or on (white) and indicates if the far-red (FR) light is on or off. The saturating pulses (F_m) are indicated. (B) qT values of WT plants acclimated to LL, NL, and HL. SD is indicated, $n \geq 4$.

Functional Effect of PSII Acclimation. To determine the effect of the antenna size on the light-harvesting and trapping capacity of PSII, we measured time-resolved fluorescence for membranes of plants acclimated to different light conditions (LL, NL, and HL). The membranes were measured in two states: state 1 (St1), in which all LHCII is associated with PSII[12]), and light-adapted state, in which part of the "extra" LHCII is associated with PSI.[14] The low-temperature fluorescence spectra and native gels of these thylakoids (see figure 1 in ref 14) show that St1 and St2 were successfully induced. The samples were excited at 440 or 475 nm. Excitation at 475 nm leads to preferential excitation of the external antenna, which coordinates large numbers of Chls b, while 440 nm excitation leads to relatively more excitations in the core, which exclusively coordinates Chl a and β-carotene. The emission was detected at 680, 700, and 720 nm; the 680 nm detection was measured twice to check the stability of the membranes. Figure 3 shows the fluorescence decay traces of LL, NL, and HL membranes after exciting the St1 samples at 475 nm and detecting at 680 nm.

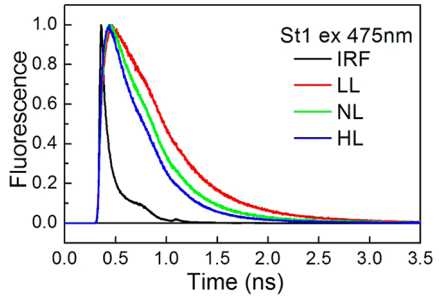

Figure 3. Fluorescence decay traces of thylakoid membranes of LL, NL, and HL plants together with the instrument response function (IRF). Excitation was at 475 nm, detection was at 680 nm, and traces are normalized to their maximum.

Clearly, the HL samples show the fastest fluorescence decay while the LL samples decay the slowest. Four lifetimes were needed to fit the fluorescence decay of each sample. As an example, Table 2 shows the fitting results for the fluorescence decay of the LL St1 thylakoids after excitation at 475 nm.

Previous work has shown that both photosystems contribute to the 70−90 ps component,[9,40,53,54] while PSII is mainly responsible for the subnanosecond components.[9] The 2 to 3 ns component can be ascribed to a small fraction of closed PSII RCs or uncoupled Chls, and this component is below 2% in our measurements. At longer detection wavelengths, the typical red emission of PSI contributes more to the fluorescence, which is reflected by the increased amplitude of the 70−90 ps component. To extract the lifetime of PSII it is necessary to determine the relative contributions of both photosystems to the 70−90 ps component. With this aim, the decay curves at the three detection wavelengths were analyzed simultaneously,

dx.doi.org/10.1021/jp401663w | J. Phys. Chem. B 2013, 117, 11200−11208

Table 2. Results of Global Fitting of Fluorescence Decay Curves of LL St1 Thylakoid Membranes[a]

	relative amplitude					DAS			
	680 nm a	680 nm b	700 nm	720 nm		680 nm a	680 nm b	700 nm	720 nm
89 ps	28.2%	28.1%	41.9%	54.3%	89 ps	0.87	0.86	0.47	0.47
0.31 ns	46.1%	45.4%	37.3%	28.9%	0.31 ns	1.43	1.39	0.42	0.25
0.58 ns	25.3%	26.1%	20.6%	16.5%	0.58 ns	0.78	0.80	0.23	0.14
3.2 ns	0.4%	0.4%	0.3%	0.3%	3.2 ns	0.01	0.01	0.00	0.00
$<\tau>$	304 ps	311 ps	249 ps	209 ps	SS fluor	1.0	1.0	0.31	0.21

[a]Excitation was at 475 nm. Detection wavelengths are as indicated. 680 nm a and 680 nm b represent the two repetitions of 680 nm detection. The average fluorescence lifetime is calculated according to $<\tau> = \Sigma A_i*\tau_i/\Sigma A_i$, where A_i is the amplitude associated with τ_i. The steady-state fluorescence (SS fluor) for each detection wavelength is given by SS fluor = $\Sigma A_i*\tau_i$, where i runs from 1 to 4 and the amplitudes A_i correspond to the height of the DAS at a particular wavelength. The SS fluorescence is normalized to 1.0 at 680 nm.

leading to the DAS. The DAS can be used to disentangle the contribution of each photosystem, taking advantage of the fact that the spectra of PSII and PSI are different with the former peaking at 680 nm and the latter at 720 nm.[55,56] The shape of the PSI ~80 ps DAS is known from studies on purified systems, for example, ref 53, and for the PSII DAS, the shape is the same as that for the subnanosecond components that are obtained from the fits.[9,40] Details of this method can be found in ref 9. The contribution of PSII to the 89 ps component at 680 nm (which is in the following indicated as q(II)), was calculated based on the 720/680 nm or 700/680 nm ratios of the PSI and PSII DAS (Table 3). By combining the PSII contribution to the

Table 3. Fluorescence Kinetics of LL St1 PSII in Thylakoid Membranes[a]

	680^a-720	680^b-720	680^a-700	680^b-700
q(II)	0.80	0.80	0.80	0.80
89 ps	24%	24%	24%	24%
0.31 ns	49%	48%	49%	48%
0.58 ns	27%	28%	27%	28%
$<\tau>$	326 ps	328 ps	326 ps	329 ps
$<\tau>$	327 ± 1.5 ps			

[a]Excitation wavelength was 475 nm. q(II) represents the relative contribution of PSII to the DAS of the fastest decay component for thylakoid membranes measured at 680 nm. It is calculated according to $q(\mathrm{II}) = ((Thyl_{720or700}/Thyl_{680}) - (PSI_{720or700}/PSI_{680}))/((PSII_{720or700}/PSII_{680}) - (PSI_{720or700}/PSI_{680}))$, where Thyl### is the amplitude of the DAS of the fastest decay component in the thylakoids (89 ps, Table ##) at the indicated wavelengths; PSI### is the amplitude of the ~80 ps PSI DAS at the indicated wavelengths, obtained from Wientjes et al. 2011, where the ratios PSI720/PSI680 and PSI700/PSI680 were 2.0 and 1.47, respectively, for excitation at 475 nm. PSII### is the relative amplitude of the PSII DAS at the indicated wavelengths, where the ratios of PSII720/PSII680 and PSII700/PSII680 were taken from the 0.31 ns thylakoid DAS (Table ##), which is a pure PSII component. The average PSII lifetime is calculated using q(II) calculated based on the $680^{a,b}$ detection in combination with 720 or 700 nm. The average lifetimes ± the standard deviation of the four values are given.

89 ps DAS with the other components, the average trapping time of PSII in the membranes is obtained. The value for LL is 327 ps, which is slightly shorter than the 339 ps previously found for PSII in WT thylakoid membranes under similar excitation conditions.[9] Indeed, a shorter lifetime is expected given that the number of LHCII trimers per PSII RC with a value of 3.1 is lower than the value of 4.0 reported for the thylakoids used in the work of van Oort et al.[9]

The fluorescence kinetics of PSII in St1 NL and HL membranes (excitation at 475 nm) were resolved in the same way as described for LL. Figure 4 shows the relative amplitudes

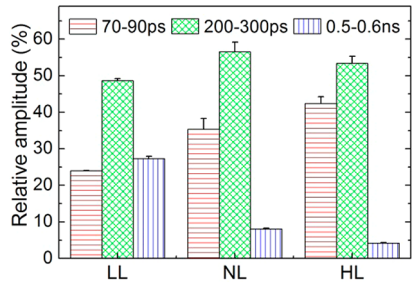

Figure 4. Relative amplitudes of PSII lifetimes of LL, NL, and HL St1 membranes; excitation was at 475 nm.

for the short (70–90 ps), middle (0.19 to 0.31 ns), and long (0.5 to 0.6 ns) PSII lifetimes. It is clear that the amplitude of the long lifetime decreases with decreasing PSII antenna size, while the relative amplitude of the short lifetime increases. In addition, the lifetimes within each group also decrease with decreasing PSII antenna size (Table 4). Together, these effects

Table 4. Fluorescence Lifetimes of PSII in Thylakoid Membranes of LL, NL, and HL Plants

	LL	NL	HL
short	89 ps	84 ps	77 ps
middle	0.31 ns	0.26 ns	0.23 ns
long	0.58 ns	0.60 ns	0.58 ns

result in a reduced average lifetime for HL PSII (179 ps) with a small antenna size and an increased average lifetime for LL PSII (327 ps) with a large antenna size, while NL PSII has a value in between (224 ps).

The same trend was observed upon excitation at 440 nm, in which there is relatively more excitation into the core as compared with the 475 nm excitation (Figure 5).

The difference in lifetime between 475 and 440 nm excitation scales with the excitation energy migration time from the antenna to the RC.[9,42] For LL, the difference is 17 ps. Note that the difference observed by van Oort et al. (2010) was similar, namely, 13 ps, which in that case corresponded to a migration time of ~150 ps. For NL and HL, we observe that the difference is smaller than the standard deviation (<5 ps) in the measurement. Apparently, the migration time in the LL thylakoids is substantially longer than that for the NL and HL thylakoids. Figure 6A shows that the relative amplitude of the

dx.doi.org/10.1021/jp401663w | J. Phys. Chem. B 2013, 117, 11200–11208

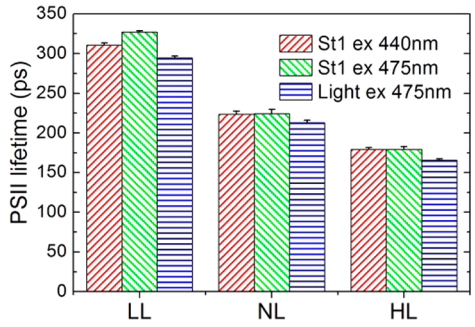

Figure 5. Average PSII excited-state lifetimes of St1 (excitation at 440 and 475) or light-adapted membranes (excitation at 475 nm). To calculate q(II), the ratios of the ~80 ps PSI DAS (PSI720/PSI680 and PSI700/PSI680) after excitation at 440 nm were taken from ref 53. For light-adapted membranes, these values were calculated based on the 80−90 ps DAS of PSI and PSI-LHCII normalized on their relative absorption cross section for excitation at 475 nm.[14] SD is indicated.

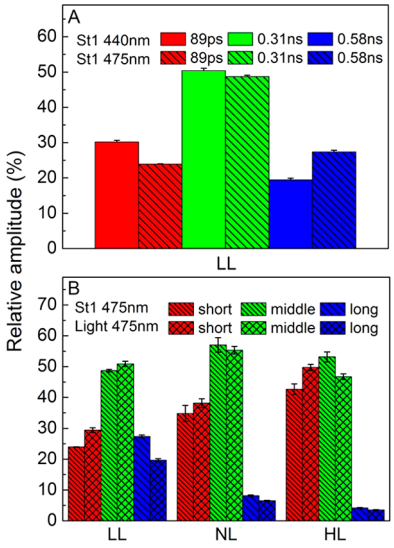

Figure 6. Relative amplitudes of PSII fluorescence decay lifetimes. (A) LL St1 thylakoid membranes, after excitation at 440 nm or 475 nm. (B) LL, NL, or HL thylakoid of St1 or light-adapted membranes.

long PSII lifetime in LL thylakoids is higher after excitation at 475 nm as compared with 440 nm. This supports the idea that the "extra" LHCII trimers, which are more abundant in LL thylakoids and which are preferentially excited at 475 nm, give a strong contribution to the slow excitation energy transfer to the core.

We have recently shown that during the day (light-adapted conditions) the antenna size of a large fraction of PSI is increased by the association of an "extra" LHCII trimer[14] and thus resembles St2. Figure 5 shows that the PSII lifetime is shorter under the light-adapted condition (when part of LHCII is associated with PSI) as compared with St1 conditions (when all LHCII is associated with PSII). In LL, the average lifetime drops from 327 ps in St1 to 295 ps under light-adapted conditions, and a similar effect is observed for NL and HL plants. Figure 6B shows that in LL membranes the relative amplitude of the slow PSII component is smaller in light-adapted plants as compared with St1, whereas in HL the main difference is found for the middle component, and for NL both the middle and the slow components are decreased in light-adapted membranes, as compared with St1. This indicates that the "extra" LHCII, which can migrate between PSI and PSII, can only transfer its excitation energy slowly to PSII in LL membranes, while the transfer is rather fast in HL membranes, suggesting a shorter distance to PSII in the latter.

DISCUSSION

Light growing conditions have a large effect on the antenna size of PSII, leading to an increase in the expression of Lhcb1 and Lhcb2 in low light and thus to an increase in the number of LHCII trimers per RC. The opposite is observed in high light, where not only the amount of LHCII trimers decreases but also the level of CP24 goes down, indicating a reduction of the antenna size of the PSII supercomplexes, as shown also by structural studies.[51] It is interesting to note that in HL the decrease in LHCII mainly affects trimer-M, which is directly associated with PSII via CP24, while the pool of extra LHCII, participating in state transitions, is still present. This is directly related to the fact that even in HL part of the LHCII is associated with PSI and this extra LHCII pool is essential to maintain the absorption balance between the two photosystems.[14]

Although the changes in the antenna size of PSII upon acclimation to different light conditions have been described in the past,[5,24,25,27,28] the consequences of the observed changes on PSII photochemical function still need to be determined.

PSII Charge-Separation Efficiency Varies from 91 to 84% Depending on the Growth Conditions. The major parameter for the functioning of PSII is the quantum yield of charge separation (Φ_{CS}), which can be calculated based on τ_{avg} (PSII total lifetime or overall trapping time) and τ_{Chl}. The excited-state lifetime of PSII in the absence of charge separation (τ_{Chl}) was recently determined to be 2 ns.[57] Using this value and the values of τ_{avg} determined in this study for LL, NL, and HL plants, we could calculate the quantum yield of charge separation (Table 5). The values range from 91% in HL, when the antenna size is small, to 84% under low-light conditions when the antenna size is rather large. It is clear that the increased light absorption cross section of the large PSII antenna in LL plants comes at the cost of decreased charge-separation efficiency. On the basis of the absorption spectrum of the $C_2S_2M_2$ supercomplex[8] and the absorption spectra and number of LHCII trimers (Table 1), it can be calculated that the total amount of absorption is 19% larger for LL PSII as compared with NL PSII. It can thus be concluded that the loss in efficiency of a few percent is largely compensated by the

Table 5. PSII Trapping Times and Efficiencies in LL, NL, and HL Thylakoids[a]

	#Chl a/PSII	τ_{trap}	τ_{mig}	τ_{avg}	Φ_{CS}[b]	F_v/F_m	F_v/F_m PSI corrected[c]
LL	127	160	151	311	84%	0.79	0.83
NL	111	140	84	224	89%	0.82	0.87
HL	96−105	122−134	45−57	179	91%	0.80	0.86

[a] τ_{avg} after 440 nm excitation. [b] For τ_{Chl}, a value of 2 ns is assumed. [c] See the text in section Time Resolved versus Fv/Fm.

dx.doi.org/10.1021/jp401663w | J. Phys. Chem. B 2013, 117, 11200−11208

larger absorption cross section; that is, the product of the number of pigments N per RC times the quantum yield Φ_{CS} still increases.

PSII Trapping Kinetics Becomes Largely Migration-Limited under Low-Light Conditions. The PSII total lifetime τ_{avg} can be considered as the sum of two lifetimes, the trapping time (τ_{trap}) and the migration time (τ_{mig}). In first approximation, τ_{trap} can be calculated based on the number of Chls *a* in PSII and in the PSII RC, the charge-separation time (τ_{CS}), the secondary charge-separation time (τ_{RP}), and the drop in free energy on primary charge separation (ΔG); see ref 9 for details and the Experimental Methods. The τ_{CS}, τ_{RP}, and ΔG values have been determined for PSII membranes BBY.[42] We used these values to calculate τ_{trap} of PSII in the LL, NL, and HL thylakoid membranes. In combination with the measured τ_{avg}, this also provides τ_{mig}, which is the difference between τ_{trap} and τ_{avg} (Table 5). This analysis shows that τ_{mig} of LL plants is twice as large as that in NL plants and three times larger than that in HL plants, whereas the difference in the number of Chls *a* is far less extreme. Thus the extra LHCIIs in LL (and to some extent NL) plants lead to a strong increase in the migration time (from ~50 ps in HL to 85 ps in NL and 150 ps in LL). This is also clearly demonstrated by plotting the average PSII lifetime of HL, NL, and LL plants against the number of Chls *a* (N) in PSII. Figure 7 shows a linear relationship between the number of PSII Chls *a* and the average PSII lifetime.

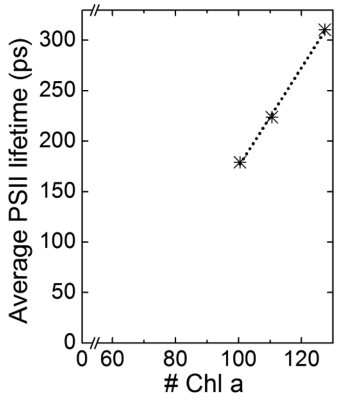

Figure 7. Average PSII lifetime versus number of Chls *a* in PSII. Points correspond to HL, NL, and LL St1 membranes; the excitation wavelength was 440 nm. The dashed line represents a linear fit of the three data points.

However, the corresponding line does not pass through the point (0,0), as might have been expected,[58] indicating that the increase in migration time for these extra Chl's is disproportionally large, suggesting an impairment of excitation energy transfer upon increasing the antenna size beyond the level of the largest supercomplex. As stated above, the product $N^*\Phi_{CS}$ nevertheless still increases upon increasing the antenna size. The maximum value of $N^*\Phi_{CS}$ is reached for N = 200−250 if the average PSII lifetime is calculated by extrapolating the straight line in Figure 7 to larger values of N, thereby providing an absolute upper limit for the optimal PSII antenna size. However, from an energetic point of view, it is not reasonable to go up to such a large antenna size because the increase in $N^*\Phi_{CS}$ is only ~7% for the final increase in size of 25%. Then, it becomes questionable whether such a relatively small increase in light-harvesting capacity per RC outweighs the extra energy cost of building additional antenna complexes.

Extra LHCII Can Efficiently Transfer Energy in HL Plants. The HL plants show a reduction in CP24 per RC of ~45%. Without CP24, trimer-M cannot bind to the PSII supercomplex,[48] thus leading to smaller PSII supercomplexes. Instead, the level of "extra" LHCIIs in HL is comparable to that of NL plants (Table 1). These "extra" LHCIIs are the mobile complexes that can migrate to PSI under St2 conditions[13] and are also associated with PSI under light-acclimated[14] conditions. Figure 6B shows that in HL plants this migration mainly leads to a decrease in the middle (0.23 ns) PSII fluorescence decay component, whereas it leads to a decrease in the long (0.58 ns) component in LL plants. Apparently, in LL plants the "extra" trimer is located further away from the PSII core, while in HL plants the absence of CP24 and trimer-M allows part of the "extra" trimers to take a position close to the core that leads to relatively fast energy transfer to the PSII RC. This situation is reminiscent of the situation in *Chlamydomonas reinhardtii*, which completely lacks CP24 but where an extra LHCII trimer is directly connected to the core on the side that in plants is occupied by CP24.[59] The "extra" LHCII in HL plants might take a similar position.

Time Resolved versus F_v/F_m. The quantum efficiency of PSII is generally approximated using the parameter F_v/F_m, for example, ref 60, although this is not universally accepted. (For recent reviews on this topic, see Schansker et al. 2013[61] and Stirbet and Govindjee 2012[62].) The observed value for optimally functioning plants is usually ~0.8,[47] and this is also the case for the plants analyzed in this work (Table 1). The value of F_v/F_m is lower than the value of the PSII quantum efficiency, as obtained by time-resolved fluorescence. This effect can to a large extent be explained by the fact that the value of F_m is not entirely due to PSII but also has a contribution from PSI fluorescence.[60] (Note that $F_v = F_m - F_o$ is entirely due to PSII because F_0 contains the same PSI contribution as F_m.) In PAM measurements from which F_v/F_m is determined, only the fluorescence above 700 nm is measured, and it contains a significant PSI contribution. The excitation at 620 nm used in the DUAL-PAM-100 excites PSI and PSII practically in the same ratio as the excitation at 440 nm, which is used for the time-resolved measurements, and the contribution of PSI can be estimated from our data. Correcting F_m for the contribution of PSI changes the value of F_v/F_m = 0.80 in HL into 0.86, still lower than the value of 0.91, as obtained from the time-resolved data. In LL, F_v/F_m = 0.79 becomes 0.83 after correction, which is relatively close to 0.84, the value obtained from the time-resolved data. The agreement is not perfect because this would require that closed PSII RCs do not cause any quenching of PSII fluorescence. However, closed PSII RCs do lead to quenching,[63−65] thereby lowering the value of F_v/F_m.

■ SUMMARY

This study relates for the first time the regulation of the LHCII antenna size of plants grown under different light intensities with the PSII operating efficiency. The data show that in low light the antenna size increases, thus increasing the absorption cross section, but this comes at the cost of a lower PSII efficiency. Instead, HL leads to smaller PSII antenna size, which allows for highly efficient PSII operation.

■ AUTHOR INFORMATION

Corresponding Author

*E-mail: R.Croce@vu.nl, Fax: +31205987999.

Present Address

[||]Emilie Wientjes: ICFO-Institut de Ciencies Fotoniques, Mediterranean Technology Park, 08860 Castelldefels (Barcelona), Spain.

Author Contributions

The manuscript was written through contributions of all authors. All authors have given approval to the final version of the manuscript.

Funding

This work was supported by The Netherlands Organisation for Scientific Research (NWO), Earth and Life Sciences (ALW), through a Vici grant (to R.C.).

Notes

The authors declare no competing financial interest.

■ ACKNOWLEDGMENTS

We thank Arie van Hoek for technical support.

■ REFERENCES

(1) Blankenship, R. E. *Molecular Mechanisms of Photosynthesis*; Blackwell Science: Malden, MA, 2002.

(2) Nelson, N.; Yocum, C. F. Structure and Function of Photosystems I and II. *Annu. Rev. Plant Biol.* **2006**, *57*, 521−565.

(3) Ballottari, M.; Girardon, J.; Dall'Osto, L.; Bassi, R. Evolution and Functional Properties of Photosystem II Light Harvesting Complexes in Eukaryotes. *Biochim. Biophys. Acta, Bioenerg.* **2012**, *1817*, 143−157.

(4) Ben-Shem, A.; Frolow, F.; Nelson, N. Crystal Structure of Plant Photosystem I. *Nature* **2003**, *426*, 630−635.

(5) Ballottari, M.; Dall'Osto, L.; Morosinotto, T.; Bassi, R. Contrasting Behavior of Higher Plant Photosystem I and II Antenna Systems During Acclimation. *J. Biol. Chem.* **2007**, *282*, 8947−8958.

(6) Dekker, J. P.; Boekema, E. J. Supramolecular Organization of Thylakoid Membrane Proteins in Green Plants. *Biochim. Biophys. Acta, Bioenerg.* **2005**, *1706*, 12−39.

(7) Yakushevska, A. E.; Jensen, P. E.; Keegstra, W.; van Roon, H.; Scheller, H. V.; Boekema, E. J.; Dekker, J. P. Supermolecular Organization of Photosystem II and its Associated Light-Harvesting Antenna in Arabidopsis thaliana. *Eur. J. Biochem.* **2001**, *268*, 6020−6028.

(8) Caffarri, S.; Kouril, R.; Kereiche, S.; Boekema, E. J.; Croce, R. Functional Architecture of Higher Plant Photosystem II Supercomplexes. *EMBO J.* **2009**, *28*, 3052−3063.

(9) van Oort, B.; Alberts, M.; de Bianchi, S.; Dall'Osto, L.; Bassi, R.; Trinkunas, G.; Croce, R.; van Amerongen, H. Effect of Antenna-Depletion in Photosystem II on Excitation Energy Transfer in Arabidopsis thaliana. *Biophys. J.* **2010**, *98*, 922−931.

(10) Peter, G. F.; Thornber, J. P. Biochemical Composition and Organization of Higher Plant Photosystem II Light-Harvesting Pigment-Proteins. *J. Biol. Chem.* **1991**, *266*, 16745−16754.

(11) Boekema, E. J.; van Roon, H.; Calkoen, F.; Bassi, R.; Dekker, J. P. Multiple Types of Association of Photosystem II and its Light-Harvesting Antenna in Partially Solubilized Photosystem II Membranes. *Biochemistry* **1999**, *38*, 2233−2239.

(12) Allen, J. F. How Does Protein-Phosphorylation Regulate Photosynthesis. *Trends Biochem. Sci.* **1992**, *17*, 12−17.

(13) Galka, P.; Santabarbara, S.; Khuong, T. T.; Degand, H.; Morsomme, P.; Jennings, R. C.; Boekema, E. J.; Caffarri, S. Functional Analyses of the Plant Photosystem I-Light-Harvesting Complex II Supercomplex Reveal That Light-Harvesting Complex II Loosely Bound to Photosystem II Is a Very Efficient Antenna for Photosystem I in State II. *Plant Cell* **2012**, *24*, 2963−2978.

(14) Wientjes, E.; van Amerongen, H.; Croce, R. LHCII is an Antenna of Both Photosystems After Long-Term Acclimation. *Biochim. Biophys. Acta, Bioenerg.* **2013**, *1827*, 420−426.

(15) Krieger-Liszkay, A. Singlet Oxygen Production in Photosynthesis. *J. Exp. Bot.* **2005**, *56*, 337−346.

(16) Barzda, V.; Peterman, E. J.; van Grondelle, R.; van Amerongen, H. The Influence of Aggregation on Triplet Formation in Light-Harvesting Chlorophyll a/b Pigment-Protein Complex II of Green Plants. *Biochemistry* **1998**, *37*, 546−551.

(17) Lampoura, S. S.; Barzda, V.; Owen, G. M.; Hoff, A. J.; van Amerongen, H. Aggregation of LHCII Leads to a Redistribution of the Triplets over the Central Xanthophylls in LHCII. *Biochemistry* **2002**, *41*, 9139−9144.

(18) Mozzo, M.; Dall'Osto, L.; Hienerwadel, R.; Bassi, R.; Croce, R. Photoprotection in the Antenna Complexes of Photosystem II - Role of Individual Xanthophylls in Chlorophyll Triplet Quenching. *J. Biol. Chem.* **2008**, *283*, 6184−6192.

(19) Carbonera, D.; Giacometti, G.; Agostini, G.; Angerhofer, A.; Aust, V. Odmr of Carotenoid and Chlorophyll Triplets in Cp43 and Cp47 Complexes of Spinach. *Chem. Phys. Lett.* **1992**, *194*, 275−281.

(20) van Mieghem, F.; Brettel, K.; Hillmann, B.; Kamlowski, A.; Rutherford, A. W.; Schlodder, E. Charge Recombination Reactions in Photosystem-II 0.1. Yields, Recombination Pathways, and Kinetics of the Primary Pair. *Biochemistry* **1995**, *34*, 4798−4813.

(21) Demmig-Adams, B.; Adams, W. W. The Role of Xanthophyll Cycle Carotenoids in the Protection of Photosynthesis. *Trends Plant Sci.* **1996**, *1*, 21−26.

(22) Horton, P.; Ruban, A. V.; Walters, R. G. Regulation Of Light Harvesting In Green Plants. *Annu. Rev. Plant Physiol. Plant Mol. Biol.* **1996**, *47*, 655−684.

(23) Johnson, M. P.; Goral, T. K.; Duffy, C. D. P.; Brain, A. P. R.; Mullineaux, C. W.; Ruban, A. V. Photoprotective Energy Dissipation Involves the Reorganization of Photosystem II Light-Harvesting Complexes in the Grana Membranes of Spinach Chloroplasts. *Plant Cell* **2011**, *23*, 1468−1479.

(24) Anderson, J. M.; Chow, W. S.; Park, Y. I. The Grand Design of Photosynthesis: Acclimation of the Photosynthetic Apparatus to Environmental Cues. *Photosynth. Res.* **1995**, *46*, 129−139.

(25) Anderson, J. M.; Andersson, B. The Dynamic Photosynthetic Membrane and Regulation of Solar-Energy Conversion. *Trends Biochem. Sci.* **1988**, *13*, 351−355.

(26) Melis, A. Dynamics of Photosynthetic Membrane-Composition and Function. *Biochim. Biophys. Acta* **1991**, *1058*, 87−106.

(27) Walters, R. G.; Horton, P. Acclimation of Arabidopsis-Thaliana to the Light Environment - Changes in Composition of the Photosynthetic Apparatus. *Planta* **1994**, *195*, 248−256.

(28) Bailey, S.; Walters, R. G.; Jansson, S.; Horton, P. Acclimation of Arabidopsis thaliana to the Light Environment: the Existence of Separate Low Light and High Light Responses. *Planta* **2001**, *213*, 794−801.

(29) Croce, R.; van Amerongen, H. Light-Harvesting and Structural Organization of Photosystem II: From Individual Complexes to Thylakoid Membrane. *J. Photochem. Photobiol., B* **2011**, *104*, 142−153.

(30) Schagger, H. Tricine-SDS-PAGE. *Nat. Protoc.* **2006**, *1*, 16−22.

(31) Hogewoning, S. W.; Wientjes, E.; Douwstra, P.; Trouwborst, G.; van Ieperen, W.; Croce, R.; Harbinson, J. Photosynthetic Quantum Yield Dynamics: From Photosystems to Leaves. *Plant Cell* **2012**, *24*, 1921−1935.

(32) Jarvi, S.; Suorsa, M.; Paakkarinen, V.; Aro, E. M. Optimized Native Gel Systems for Separation of Thylakoid Protein Complexes: Novel Super- and Mega-Complexes. *Biochem. J.* **2011**, *439*, 207−214.

(33) Wientjes, E.; Oostergetel, G. T.; Jansson, S.; Boekema, E. J.; Croce, R. The Role of Lhca Complexes in the Supramolecular Organization of Higher Plant Photosystem I. *J. Biol. Chem.* **2009**, *284*, 7803−7810.

(34) Bailleul, B.; Cardol, P.; Breyton, C.; Finazzi, G. Electrochromism: a Useful Probe to Study Algal Photosynthesis. *Photosynth. Res.* **2010**, *106*, 179−189.

(35) Cardol, P.; Bailleul, B.; Rappaport, F.; Derelle, E.; Beal, D.; Breyton, C.; Bailey, S.; Wollman, F. A.; Grossman, A.; Moreau, H.; Finazzi, G. An Original Adaptation of Photosynthesis in the Marine Green Alga Ostreococcus. *Proc. Natl. Acad. Sci. U.S.A.* **2008**, *105*, 7881−7886.

(36) Chow, W. S.; Fan, D. Y.; Oguchi, R.; Jia, H.; Losciale, P.; Park, Y. I.; He, J.; Oquist, G.; Shen, Y. G.; Anderson, J. M. Quantifying and Monitoring Functional Photosystem II and the Stoichiometry of the Two Photosystems in Leaf Segments: Approaches and Approximations. *Photosynth. Res.* **2012**, *113*, 63−74.
(37) Joliot, P.; Delosme, R. Flash-Induced 519 nm Absorption Change in Green Algae. *Biochim. Biophys. Acta* **1974**, *357*, 267−284.
(38) Croce, R.; Canino, G.; Ros, F.; Bassi, R. Chromophore Organization in the Higher-Plant Photosystem II Antenna Protein CP26. *Biochemistry* **2002**, *41*, 7334−7343.
(39) Somsen, O. J.; Keukens, L. B.; de Keijzer, M. N.; van Hoek, A.; van Amerongen, H. Structural Heterogeneity in DNA: Temperature Dependence of 2-aminopurine Fluorescence in Dinucleotides. *ChemPhysChem* **2005**, *6*, 1622−1627.
(40) Broess, K.; Trinkunas, G.; van der Weij-de Wit, C. D.; Dekker, J. P.; van Hoek, A.; van Amerongen, H. Excitation Energy Transfer and Charge Separation in Photosystem II Membranes Revisited. *Biophys. J.* **2006**, *91*, 3776−86.
(41) van Amerongen, H.; Valkunas, L.; van Grondelle, R. *Photosynthetic Excitons*; World Scientific Publishing: River Edge, NJ, 2000.
(42) Broess, K.; Trinkunas, G.; van Hoek, A.; Croce, R.; van Amerongen, H. Determination of the Excitation Migration Time in Photosystem II - Consequences for the Membrane Organization and Charge Separation Parameters. *Biochim. Biophys. Acta, Bioenerg.* **2008**, *1777*, 404−409.
(43) Passarini, F.; Wientjes, E.; Hienerwadel, R.; Croce, R. Molecular Basis of Light Harvesting and Photoprotection in CP24: Unique Features of the Most Recent Antenna Complex. *J. Biol. Chem.* **2009**, *284*, 29536−29546.
(44) Eijckelhoff, C.; Dekker, J. P. Determination of the Pigment Stoichiometry of the Photochemical-Reaction Center of Photosystem-II. *Biochim. Biophys. Acta, Bioenerg.* **1995**, *1231*, 21−28.
(45) Miloslavina, Y.; Szczepaniak, M.; Muller, M. G.; Sander, J.; Nowaczyk, M.; Rogner, M.; Holzwarth, A. R. Charge Separation Kinetics in Intact Photosystem II Core Particles is Trap-limited. A Picosecond Fluorescence Study. *Biochemistry* **2006**, *45*, 2436−2442.
(46) Bjorkman, O.; Demmig, B. Photon Yield of O-2 Evolution and Chlorophyll Fluorescence Characteristics at 77-K among Vascular Plants of Diverse Origins. *Planta* **1987**, *170*, 489−504.
(47) Adams, W. W.; Demmig-Adams, B.; Winter, K.; Schreiber, U. The Ratio of Variable to Maximum Chlorophyll Fluorescence from Photosystem-II, Measured in Leaves at Ambient-Temperature and at 77k, as an Indicator of the Photon Yield of Photosynthesis. *Planta* **1990**, *180*, 166−174.
(48) Kovacs, L.; Damkjaer, J.; Kereiche, S.; Ilioaia, C.; Ruban, A. V.; Boekema, E. J.; Jansson, S.; Horton, P. Lack of the Light-Harvesting Complex CP24 Affects the Structure and Function of the Grana Membranes of Higher Plant Chloroplasts. *Plant Cell* **2006**, *18*, 3106−20.
(49) Dainese, P.; Bassi, R. Subunit Stoichiometry of the Chloroplast Photosystem-Ii Antenna System and Aggregation State of the Component Chlorophyll-a/B Binding-Proteins. *J. Biol. Chem.* **1991**, *266*, 8136−8142.
(50) Hankamer, B.; Nield, J.; Zheleva, D.; Boekema, E.; Jansson, S.; Barber, J. Isolation and Biochemical Characterisation of Monomeric and Dimeric Photosystem II Complexes from Spinach and their Relevance to the Organisation of Photosystem II in vivo. *Eur. J. Biochem.* **1997**, *243*, 422−429.
(51) Kouril, R.; Wientjes, E.; Bultema, J.; Croce, R.; Boekema, E. High-light vs. Low-light: Effect of Light Acclimation on Photosystem II Composition and Organization in Arabidopsis thaliana. *Biochim. Biophys. Acta, Bioenerg.* **2013**, *1827*, 411−419.
(52) Mishra, Y.; Jankanpaa, H. J.; Kiss, A. Z.; Funk, C.; Schroder, W. P.; Jansson, S. Arabidopsis Plants Grown in the Field and Climate Chambers Significantly Differ in Leaf Morphology and Photosystem Components. *BMC Plant Biol.* **2012**, 12.
(53) Wientjes, E.; van Stokkum, I. H. M.; van Amerongen, H.; Croce, R. The Role of the Individual Lhcas in Photosystem I Excitation Energy Trapping. *Biophys. J.* **2011**, *101*, 745−754.
(54) Ihalainen, J. A.; van Stokkum, I. H. M.; Gibasiewicz, K.; Germano, M.; van Grondelle, R.; Dekker, J. P. Kinetics of Excitation Trapping in Intact Photosystem I of Chlamydomonas reinhardtii and Arabidopsis thaliana. *Biochim. Biophys. Acta, Bioenerg.* **2005**, *1706*, 267−275.
(55) Franck, F.; Juneau, P.; Popovic, R. Resolution of the Photosystem I and Photosystem II Contributions to Chlorophyll Fluorescence of Intact Leaves at Room Temperature. *Biochim. Biophys. Acta, Bioenerg.* **2002**, *1556*, 239−246.
(56) Croce, R.; Dorra, D.; Holzwarth, A. R.; Jennings, R. C. Fluorescence Decay and Spectral Evolution in Intact Photosystem I of Higher Plants. *Biochemistry* **2000**, *39*, 6341−6348.
(57) Belgio, E.; Johnson, M. P.; Juric, S.; Ruban, A. V. Higher Plant Photosystem II Light-Harvesting Antenna, Not the Reaction Center, Determines the Excited-State Lifetime-Both the Maximum and the Nonphotochemically Quenched. *Biophys. J.* **2012**, *102*, 2761−2771.
(58) van Amerongen, H.; Dekker, J. *Light-Harvesting Antennas in Photosynthesis*; Kluwer Academic Publishers: Dordrecht, 2003; pp 219−251.
(59) Tokutsu, R.; Kato, N.; Bui, K. H.; Ishikawa, T.; Minagawa, J. Revisiting the Supramolecular Organization of Photosystem II in Chlamydomonas reinhardtii. *J. Biol. Chem.* **2012**, *287*, 31574−31581.
(60) Baker, N. R. Chlorophyll Fluorescence: A Probe of Photosynthesis in vivo. *Annu. Rev. Plant Biol.* **2008**, *59*, 89−113.
(61) Schansker, G.; Toth, S. Z.; Holzwarth, A. R.; Garab, G. Chlorophyll a Fluorescence: Beyond the Limits of the QA Model. *Photosynth. Res.* **2013**, DOI: 10.1007/s11120-013-9806-5.
(62) Stirbet, A.; Govindjee. Chlorophyll a Fluorescence Induction: a Personal Perspective of the Thermal Phase, the J-I-P Rise. *Photosynth. Res.* **2012**, *113*, 15−61.
(63) Schatz, G. H.; Brock, H.; Holzwarth, A. R. Kinetic and Energetic Model for the Primary Processes in Photosystem-II. *Biophys. J.* **1988**, *54*, 397−405.
(64) Gilmore, A. M.; Shinkarev, V. P.; Hazlett, T. L. Govindjee, Quantitative Analysis of the Effects of Intrathylakoid pH and Xanthophyll Cycle Pigments on Chlorophyll a Fluorescence Lifetime Distributions and Intensity in Thylakoids. *Biochemistry* **1998**, *37*, 13582−13593.
(65) Holzwarth, A. R.; Miloslavina, Y.; Nilkens, M.; Jahns, P. Identification of two Quenching Sites Active in the Regulation of Photosynthetic Light-Harvesting Studied by Time-Resolved Fluorescence. *Chem. Phys. Lett.* **2009**, *483*, 262−267.